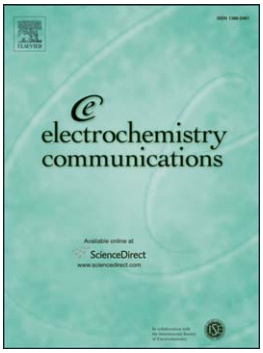

Extracellular electron transfer of biocathodes: Revealing the potentials for nitrate and nitrite reduction of denitrifying microbiomes dominated by *Thiobacillus* sp.

Narcís Pous, Christin Koch, Jesús Colprim, Sebastià Puig, Falk Harnisch

PII: S1388-2481(14)00329-4
DOI: doi: 10.1016/j.elecom.2014.10.011
Reference: ELECOM 5299

To appear in: *Electrochemistry Communications*

Received date: 25 September 2014
Revised date: 21 October 2014
Accepted date: 21 October 2014

Please cite this article as: Narcís Pous, Christin Koch, Jesús Colprim, Sebastià Puig, Falk Harnisch, Extracellular electron transfer of biocathodes: Revealing the potentials for nitrate and nitrite reduction of denitrifying microbiomes dominated by *Thiobacillus* sp., *Electrochemistry Communications* (2014), doi: 10.1016/j.elecom.2014.10.011

Extracellular electron transfer of biocathodes: Revealing the potentials for nitrate and nitrite reduction of denitrifying microbiomes dominated by *Thiobacillus* sp.

Narcís Pous[a]; Christin Koch[b]; Jesús Colprim[a]; Sebastià Puig [a]; Falk Harnisch[b,*]

[a]LEQUiA, Institute of the Environment, University of Girona, C/ Maria Aurèlia Capmany, 69, Facultat de Ciències, E-17071 Girona, Spain.

[b]Helmholtz Centre for Environmental Research - UFZ, Department of Environmental Microbiology, Permoserstraße 15 I 04318 Leipzig, Germany.

[*] Corresponding author: (F. Harnisch)

E-mail address: falk.harnisch@ufz.de
Tel.: +49 341 235 - 1337

Abstract

The use of biocathodes in bioelectrochemical systems (BES) for the removal of nitrate in wastewater has become a vital field of research. However, the elucidation of the underlying extracellular electron transfer (EET) fundamentals of denitrifying biocathodes is still lacking, but required for a deeper BES understanding and engineering. This study reports for the first time on the thermodynamics of microbial cathodes for nitrate and nitrite reductions using microbial microcosms isolated from a running denitrifying BES. Cyclic voltammetry showed that nitrate and nitrite reduction proceed at -0.30V, and -0.70V vs. Ag/AgCl, respectively, by surface associated EET sites. The biocathodes were predominantly covered by *Thiobacillus* sp. contributing with a nitrate reductase (narG) to the major function of the microscosms. In conclusion, the EET characteristics of denitrifying biocathodes are demonstrated for the first time.

Keywords:

Autotrophic biological denitrification, bioelectrochemical system, cyclic voltammetry, microbial electrochemical technology, nitrate reductase, nitrogen removal.

1. Introduction

The removal of nitrate (NO_3^-) from wastewater is a worldwide concern [1]. Conventional treatments based on biologic heterotrophic denitrification (i.e. organic carbon as bacterial carbon source) are often limited by the availability of the electron donor [2]. Alternatively cathodes of bioelectrochemical systems (BES) are considered as a safe and endless source of electrons for autotrophic microbial nitrate reduction with inorganic carbon being the only microbial carbon source [3, 4].

So far, research efforts have been focused on optimizing operational parameters of denitrifying-BES (d-BES). The influence of the cathode potential [5], the pH [6], or the conductivity [7] were assessed and microbial community analyses was shown a highly diverse community, suggesting a potential key role of *Proteobacteria* [8]. In addition to the only scattered information from the engineering perspective, the underlying fundamentals of the microbial extracellular electron transfer (EET) are still untapped.

The EET of denitrifying bacteria depends on the thermodynamics of the involved four reduction steps [9] (eq.1, shown vs. Ag/AgCl and pH 8).

$$NO_3^- \xrightarrow[2H^+ + 2e^-]{E=+0.17V} NO_2^- \xrightarrow[2H^+ + 1e^-]{E=+0.07V} NO \xrightarrow[1H^+ + 1e^-]{E=+0.92V} 1/2N_2O \xrightarrow[1H^+ + 1e^-]{E=+1.10V} 1/2N_2 \quad \text{(eq1)}$$

The midpoint potentials (E_m, respectively formal potentials) of isolated denitrifying enzymes of specific microbial species were elucidated. Nitrate reductase GHI [10], Cu nitrite reductase [11] and Cu nitrous oxide reductase [12] presented potentials of -0.19V, -0.07V and -0.14V (vs. Ag/AgCl), respectively. However, nothing is known on the EET of denitrifying biocathodes.

Within this communication we report on the EET characteristics of denitrifying biocathodes using microcosms, i.e. an artificial simplified ecosystem, isolated from a running denitrifying-BES, allowing detailed cyclic voltammetric, physiological and

molecular biological analysis. This study focuses on the reduction of nitrate to nitrite as a model process, but certainly, the generation of further reduced products (like greenhouse gases NO and N_2O) is of enormous relevance, e.g. for greenhouse gas emissions.

2. Materials and methods

2.1. Experimental set-up

The experiments were carried out in tailor-made single-chamber bioelectrochemical cells (microcosms). Each microcosm (Figure 1) possessing a final net-volume of 18 mL was assembled with two graphite rods (CP-Graphite GmbH, Germany) possessing projected surface areas of 6.2cm^2 and 7.0cm^2 for working and counter electrodes, respectively, being connected with stainless steel wires and one Ag/AgCl reference electrode (sat. KCl, SE11 Sensortechnik Meinsberg, Germany). If not stated otherwise, all potentials in this communication are provided vs. Ag/AgCl(sat. KCl; +0.197V vs. standard hydrogen electrode (SHE)).

Four different media were used at pH 8 and room temperature (22ºC). All media were prepared with distillate water and flushed with N_2 gas. They all contained 0.500$g\cdot L^{-1}$NaCl, 0.100$g\cdot L^{-1}$ $MgSO_4\cdot 7H_2O$, 0.015$g\cdot L^{-1}$ $CaCl_2$, 0.020$g\cdot L^{-1}$ NH_4Cl, 1.000$g\cdot L^{-1}$ $NaHCO_3$, 1.547$g\cdot L^{-1}$ $Na_2HPO_4\cdot 7H_2O$, 0.584$g\cdot L^{-1}$ KH_2PO_4 and 1$mL\cdot L^{-1}$ of microelements solution [13]. In addition, either NO_3^-(14.28$mmolNO_3^-\cdot L^{-1}$; equivalent to 885$mgNO_3^-\cdot L^{-1}$) or NO_2^-(7.14$mmolNO_2^-\cdot L^{-1}$; equivalent to 328$mgNO_2^-\cdot L^{-1}$) or NO_3^- +NO_2^-(14.28$mmolNO_3^-\cdot L^{-1}$ and 7.14$mmolNO_2^-\cdot L^{-1}$) was added. The concentration were chosen, as there are typical for d-BES research and represent equivalent nitrogen concentrations of 200$mg^-\cdot L^{-1}$ for NO_3^- and 100$mg^-\cdot L^{-1}$ for NO_2^-, respectively.

2.2. Inoculation and operation

The microcosms were inoculated from the cathode of a running 1L d-BES possessing a packed-bed cathode (similar to [14]). The d-BES overall performance was known, but a preliminary computational fluid dynamics study (data not shown) demonstrated that spatial heterogeneity existed. Consequently, inoculums were taken from three different sampling ports of the cathode volume (denominated as SP1, SP2, SP3; Figure 1) and from the effluent (SCat) using a needle to scratch the electrode surface and drawing a total volume of 2mL. Drawn volume was immediately inoculated anoxic into a microcosm with 16mL of NO_3^- containing medium (Figure 1). Two independent series of inoculation were performed with similar results; the results of the second run are shown here.

The working electrode of each microcosm was operated chronoamperometrically (CA) at -0.32V (identical to the parent d-BES, which was operated at a fixed cathode potential of -0.32V). Once stable reductive current density was reached (-2.45, -3.60, -3.49 and -3.78 $\mu A \cdot cm^{-2}$ for SCat, SP1, SP2 and SP3, respectively), microcosms were exposed sequentially to media containing i) NO_3^-+NO_2^-; ii) NO_3^-; iii) NO_2^-; iv) NO_3^- and v) to buffer solution. Cyclic voltammetry (CV) was performed and three cycles were recorded from 0.0 to -0.8V at scan rate of 0.5 $mV \cdot s^{-1}$. The third cycle, showing a steady-state performance, was used for data analysis in accordance to [15]. The coulombic efficiency (CE) for nitrate reduction to nitrite was calculated considering the consumption of two moles of electrons per mol of reduced nitrate.

2.3. Analytical methods

Nitrate and nitrite were analyzed using photometric tests (114563 NO_3^-Spectroquant® and 100609 NO_2^-spectroquant®; Merck, Germany).

2.4. Microbiological analyses

Terminally, the electrodes were stored at -20°C. DNA was extracted according to [16]. PCR amplification of 16S rDNA and functional denitrification genes was done according to [16] and [17].Representative samples were further cloned and sequenced.

3. Results and discussion

3.1. Performance of denitrifying microcosms

Microcosms performances, including current consumption, accumulated charge, nitrate reduction and *CE*, are summarized in Table 1. Low heterogeneity among the microcosms was observed and SP1, SP2 and SP3 microcosms showed similar stable reduction current (-3.60, -3.49 and -3.78 $\mu A \cdot cm^{-2}$), while Scat was less active (-2.45$\mu A \cdot cm^{-2}$). The nitrate removal correlated positively with the current density, showing Spearmann's correlation of 0.764.

Commonly, nitrite accumulated in all microcosms (between 34.4% and 54.1% of reduced nitrate), indicating a higher reduction from NO_3^- to NO_2^- than further from NO_2^-, being well in line with the CV-results that show that a more negative potential is needed for nitrite reduction (see below). The derived *CE* of NO_3^- reduction to NO_2^- varied between 24.5% and 46.9%. In summary, this data shows that well-working denitrifying, in terms of nitrate removal, biocathode microcosms were established.

3.2. Cyclic voltammetry analysis of the microcosms

Once stable current in growth media was reached, microcosms were tested at different conditions, *i.e.* media containing NO_3^-, NO_3^-+NO_2^-, NO_2^- or buffer. The periodical change of media implied that suspended biomass was removed from the set-up and thus, the bioelectrochemical activity can be assigned to microorganisms attached to the electrode (biofilm). All results are summarized in Table 1 and Figure 2

The current density of all microcosms was highest, when being exposed to a nitrate solution, followed by nitrate plus nitrite and nitrite. For all microcosms no reduction current was observed for buffer solution, demonstrating the need for NO_3^- and/ or NO_2^- to serve as electron acceptor.

In NO_3^-containing media, the microcosms presented a similar sigmoidal shape of the CV, *i.e.* showing bioelectrocatalysis, with an inflection point (maximum of the first derivative) of the EET-site of E_1= -0.30V (Fig. 2 A-D). This formal potential could be related not only to nitrate reduction, but also to the simultaneous reduction of nitrate and nitrite sequential reductions to N_2 (through NO_2^- and N_2O), which was also confirmed by chemical analyses described in section 3.1. When exposing the biofilm electrodes to NO_3^-plus NO_2^- media the reductive current density in the chronoamperometry decreased in comparison to media containing only NO_3^-. Remarkably, the E_1 at -0.30V was stable, but a double-sigmoidal shape of the CV-curve was found with a second EET-site at E_2 = -0.70V. When only nitrite (and no nitrate) was present as electron acceptor, electrodes in the microcosms showed only one reductive peak at -0.70V (Fig 2 A-D). These results clearly show that E_1 =-0.30V represents nitrate to nitrite reduction and E_2 = -0.70 V nitrite reduction. The NO_2^- reduction signal, being (at identical concentration) higher in the absence of NO_3^-, points to the competition between denitrifying enzymes respectively an inhibition of nitrate reduction at too high nitrite concentrations [18,19].

In conventional heterotrophic denitrification the accumulation of denitrification intermediates could be related not only to a lack of electron donor, but also to the electron competition between denitrifying enzymes when the whole denitrifying pathway is performed within the same microorganism [19]. We assume that in the evaluated biofilms, nitrate reductase(s) used electrons more efficiently, which can also be explained by its operating potential of -0.32V that is triggering the build-up of EET-sites catalyzing the first reaction step.

Redox-peaks for non-turnover CVs, allowing a further characterization of the EET mechanism [20], were also detected (Fig 2. E-H) – a finding hardly reported for biocathodes, so far [21]. First, a redox couple with a midpoint potential between -0.24V and -0.29V and, secondly, an oxidative peak between -0.40V and -0.44Vwere exhibited by all electrodes. The more positive redox centers can be related to the nitrate reduction (being related to E_1), whereas the more negative single oxidation peak to the nitrite reduction. For the first redox couple the small shift to more positive values (in comparison to the turn-over signal) could be related to the small local pH-gradients. This provides further evidence that the two reaction steps of nitrate reduction and nitrite reduction are catalyzed by two different redox moieties. However, the only very small current densities, even at low scan rates, as well as the lack of the corresponding reductive peak for the more negative redox systems aggravates any detailed analysis, so far.

The sequence of the potentials for nitrate reduction (E_1=-0.30V) and nitrite reduction (E_2=-0.70V) were in line with their standard potentials, being corrected for experimental conditions (pH 8 and 22ºC) were +0.17V and +0.07V vs. Ag/AgCl for NO_3^-/NO_2^- and NO_2^-/NO, respectively [9]. The resulting difference between the mid-point potential in the turn-over CV curve and the standard redox potential of the reaction in the

biocathodes, approximating the respective overpotentials at 50% of maximum current density, were -0.47V for NO_3^-/NO_2^- and -0.77V for NO_2^-/NO.

The use of porous electrode in the d-BES' cathode (granular graphite) implies a heterogeneous distribution of the cathode potential [22] that may allow the simultaneous reduction of NO_3^- and NO_2^-.

3.3. Microbiome of the microcosms

The microbiological analyses revealed that the biofilms were predominantly (75-80%) composed of the betaproteobacterium *Thiobacillus* sp. (highest BLAST hit for cultured representative *Thiobacillus thiophilus* strain D24TN, 99% identity). *Thiobacillus* sp. have been described as bacteria able to reduce nitrate through Fe(II) oxidation, which contributes to the geochemical iron cycling [23]. Furthermore, electric currents through natural conductive minerals have been demonstrated between *Geobacter sulfurreducens* and *Thiobacillus denitrificans*, showing the EET-ability and suggesting *Thiobacillus* eletrotroph capability [24]. Additional analyses of the functional genes supported the dominance of *Thiobacillus* in the microcosms. The predominant narG gene, encoding for respiratory nitrate reductases (narGHI), showed highest similarly to *Thiobacillus denitrificans* ATCC 25259 (highest BLAST hit for cultured representative, 85% identity). Redox potentials of the respective enzyme have been elucidated at about +7mV vs. SHE for narGHI complexes, respectively [10,25]. In our work, the reduction potential for nitrate was found at -0.30V vs. Ag/AgCl (i.e. -103mV vs. SHE), which further substantiates the electron transfer from the electrode to the enzyme.

Further amplification products of functional denitrification enzymes showed either no significant similarity to present sequences in the database (nirK) or affiliated to low abundant members of the microbiomes (napA, nirS, nosZ) indicating their presence but limited contribution to the microbiome function.

4. Conclusions

This communication demonstrated, for the first time, the EET characteristics of a denitrifying biocathode. Microcosms isolated from a running denitrifying-BES were

successfully used for studying of EET thermodynamics as well as microbiome analyses. CV analysis for a denitrifying biocathode showed nitrate reduction to nitrite proceeds at -0.30V and nitrite reduction at -0.70V. Microbiome analyses showed the dominance of *Thiobacillus* sp. and its respiratory nitrate reductases (narGHI), suggesting a key role on the bioelectrochemical reduction of nitrate and nitrite.

The presented results allow a better understanding of EET fundamentals of denitrifying cathodes based on *Thiobacillus* sp. in BES and thus can contribute to their engineering in order to start-up and operate denitrifying bioelectrochemical systems, e.g. nitrate removal rates depending on the cathode potential. Further, the here exploited strategy of using microcosms can be adapted further, e.g. studying the generation of further reduced nitrogen species (like N_2O) or their pH-/ temperature dependency respectively studying heterogeneities in packed electrodes by using distinctive potentials for biofilm growth, or reactions of further microbial electrodes.

Acknowledgements

The authors acknowledge the scientific assistance of Prof. M.D. Balaguer. F.H. acknowledges support by the BMBF (Research Award "Next generation biotechnological processes – Biotechnology 2020+") and the Helmholtz-Association (Young Investigators Group). This work was supported by the Helmholtz-Association within the Research Programme Terrestrial Environment and the Spanish Government (CTQ2011-23632). N.P. was supported by the Catalan Government (2012FI-B00941) and the University of Girona (MOB2014-ref22).

References

[1] P.M. Vitousek, J.D. Aber, R.W. Howarth, G.E. Likens, P.A. Matson, D.W. Schindler, W.H. Schlesinger, D.G. Tilman, Human alteration of the global nitrogen cycle: sources and consequences, Ecol. Appl. 7 (1997) 737–50. DOI: 10.2307/2269431.

[2] V. Matějů, S. Čižinská, J. Krejčí, T. Janoch, Biological water denitrification - A review, Enzyme Microb. Technol. 14 (1992) 170–83. DOI: 10.1016/0141-0229(92)90062-S.

[3] P. Clauwaert, K. Rabaey, P. Aelterman, L. De Schamphelaire, T.H. Pham, P. Boeckx, N. Boon, W. Verstraete, Biological denitrification in microbial fuel cells, Environ. Sci. Technol. 41 (2007) 3354–60. DOI: 10.1021/es062580r.

[4] K.B. Gregory, D.R. Bond, D.R. Lovley, Graphite electrodes as electron donors for anaerobic respiration, Environ. Microbiol. 6 (2004) 596–604. DOI: 10.1111/j.1462-2920.2004.00593.x.

[5] B. Virdis, K. Rabaey, Z. Yuan, R.A. Rozendal, J. Keller, Electron fluxes in a microbial fuel cell performing carbon and nitrogen removal, Environ. Sci. Technol. 43 (2009) 5144–9. DOI: 10.1021/es8036302.

[6] P. Clauwaert, J. Desloover, C. Shea, R. Nerenberg, N. Boon, W. Verstraete, Enhanced nitrogen removal in bio-electrochemical systems by pH control, Biotechnol. Lett. 31 (2009) 1537–43. DOI: 10.1007/s10529-009-0048-8.

[7] S. Puig, M. Coma, J. Desloover, N. Boon, J. Colprim, M.D. Balaguer, Autotrophic denitrification in microbial fuel cells treating low ionic strength waters, Environ. Sci. Technol. 46 (2012) 2309–15. DOI: 10.1021/es2030609.

[8] K.C. Wrighton, B. Virdis, P. Clauwaert, S.T. Read, R.A. Daly, N. Boon, Y. Piceno, G.L. Andersen, J.D. Coates, K. Rabaey, Bacterial community structure corresponds to performance during cathodic nitrate reduction, ISME J. 4 (2010) 1443–55. DOI: 10.1038/ismej.2010.66.

[9] S.J. Ferguson, D.J. Richardson, The enzymes and bioenergetics of bacterial nitrate, nitrite, nitric oxide and nitrous oxide respiration, Chapter 8, Pages 169-206, in: D. Zannoni, Respiration in archaea and bacteria, advances in photosynthesis and respiration volume 16, Springer, Netherlands, 2004.

[10] L.J. Anderson, D.J. Richardson, J.N. Butt, Catalytic protein film voltammetry from a respiratory nitrate reductase provides evidence for complex electrochemical modulation of enzyme activity, Biochem. 40 (2001) 11294–307. DOI: 10.1021/bi002706b.

[11] H.J. Wijma, L.J.C. Jeuken, M.P. Verbeet, F.A. Armstrong, G.W. Canters, A random-sequential mechanism for nitrite binding and active site reduction in copper-containing nitrite reductase, J. Biol. Chem. 281 (2006) 16340–6. DOI: 10.1074/jbc.M601610200.

[12] S. Dell'Acqua, S.R. Pauleta, P.M.P. De Sousa, E. Monzani, L. Casella, J.J.G. Moura, I. Moura, A new CuZ active form in the catalytic reduction of N_2O by nitrous oxide reductase from *Pseudomonas nautica*, J. Biol. Inorg. Chem. 15 (2010) 967–76. DOI: 10.1007/s00775-010-0658-6.

[13] K. Rabaey, W. Ossieur, M. Verhaege, W. Verstraete, Continuous microbial fuel cells convert carbohydrates to electricity, Water Sci. Technol. 52 (2005) 515–23.

[14] N. Pous, S. Puig, M. Coma, M.D. Balaguer, J. Colprim, Bioremediation of nitrate-polluted groundwater in a microbial fuel cell, J. Chem. Technol. Biotechnol. 88 (2013) 1690-6. DOI: 10.1002/jctb.4020.

[15] F. Harnisch, S. Freguia, A basic tutorial on cyclic voltammetry for the investigation of electroactive microbial biofilms, Chem. Asian J. 7 (2012) 466–75. DOI: 10.1002/asia.201100740.

[16] C. Koch, S. Günther, A.F. Desta, T. Hübschmann, S. Müller, Cytometric fingerprinting for analyzing microbial intracommunity structure variation and identifying subcommunity function, Nat. Protoc. 8 (2013) 190–202. DOI: 10.1038/nprot.2012.149.

[17] A. Vilar-Sanz, S. Puig, A. García-Lledó, R. Trias, M.D. Balaguer, J. Colprim, L. Bañeras, Denitrifying bacterial communities affect current production and nitrous oxide accumulation in a microbial fuel cell, PLoS One. 8 (2013) e63460. DOI: 10.1371/journal.pone.0063460.

[18] Y. Pan, B.-J. Ni, P.L. Bond, L. Ye, Z. Yuan, Electron competition among nitrogen oxides reduction during methanol-utilizing denitrification in wastewater treatment, Water Res. 47 (2013) 3273–81. DOI: 10.1016/j.watres.2013.02.054.

[19] H.J. Lu, K. Chandran, Factors promoting emissions of nitrous oxide and nitric oxide from denitrifying sequencing batch reactors operated with methanol and ethanol as electron donors, Biotechnol. Bioeng. 106 (2010) 390–98. DOI: 10.1002/bit.22704.

[20] K. Fricke, F. Harnisch, U. Schröder, On the use of cyclic voltammetry for the study of anodic electron transfer in microbial fuel cells, Energy Environ. Sci. 1 (2008) 144-7. DOI: 10.1039/b802363h.

[21] M. Rosenbaum, F. Aulenta, M. Villano, L.T. Angenent, Cathodes as electron donors for microbial metabolism: which extracellular electron transfer mechanisms are involved?, Bioresour. Technol. 102 (2011) 324–33. DOI: 10.1016/j.biortech.2010.07.008.

[22] T. Doherty, J.G. Sunderland, E.P.L. Roberts, D.J. Pickett, An improved model of potential and current distribution within a flow-through porous electrode, Electrochim. Acta 41 (1996) 519–26. DOI: 10.1016/0013-4686(96)81774-9.

[23] K.L. Straub, M. Benz, B. Schink, F. Widdel, Anaerobic, nitrate-dependent microbial oxidation of ferrous iron, Appl. Environ. Microbiol. 62 (1996) 1458–60.

[24] S. Kato, K. Hashimoto, K. Watanabe, Microbial interspecies electron transfer via electric currents through conductive minerals, Proc. Natl. Acad. Sci. U.S.A. 109 (2012) 10042–6. DOI: 10.1073/pnas.1117592109.

[25] P. Bertrand, B. Frangioni, S. Dementin, M. Sabaty, P. Arnoux, B. Guigliarelli, D. Pignol, C. Léger, Effects of slow substrate binding and release in redox enzymes: theory and application to periplasmic nitrate reductase, J. Phys. Chem. B. 111 (2007) 10300–11. DOI: 10.1021/jp074340j.

A

d-BES performance at sampling		
Parameter	Units	Value
Current density	($mA\ L^{-1}_{NCC}$)	-23.9±1.4
NO_3^- reduction rate	($mmol NO_3^-\ L^{-1}_{NCC}\ d^{-1}$)	9.2±0.5
NO_2^- reduction rate	($mmol NO_2^-\ L^{-1}_{NCC}\ d^{-1}$)	1.2±0.6
Effluent [NO_3^-]	($mmol NO_3^-\ L^{-1}$)	7.4±0.9
Effluent [NO_2^-]	($mmol NO_2^-\ L^{-1}$)	6.5±0.6
CE NO_3^-/N_2	(%)	91±12

B

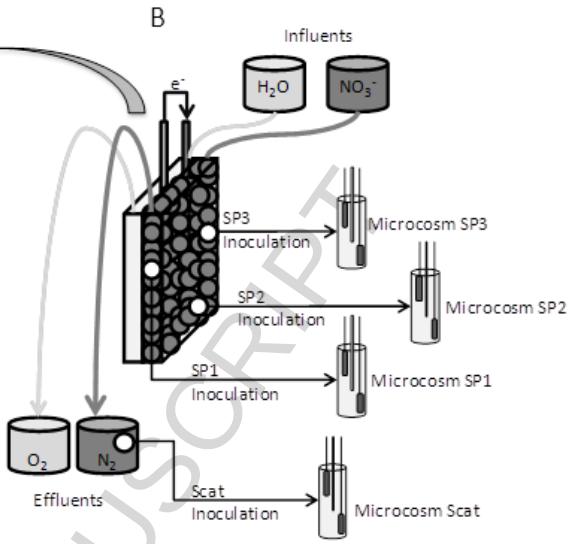

Figure 1. A) Overall d-BES performance at sampling days; NCC = net volume of the cathode compartment; CE NO_3^-/N_2 = Coulumbic efficiency of the whole denitrifying process considering the consumption of 2 moles of electrons per mol of reduced nitrate, 2 moles of electrons per mol of reduced nitrite and 2 moles of electrons per mol of reduced nitrous oxide; B) Scheme of the microcosms inoculation procedure.

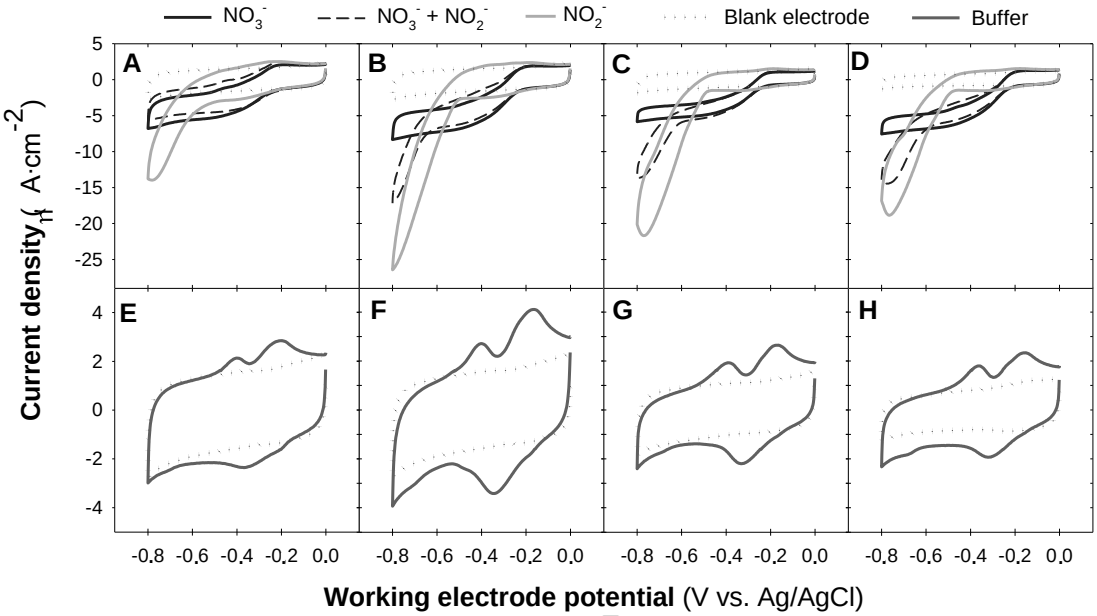

Figure 2. Panel with CVs at 0.5 mV $s^{-1}$of each microcosm at each applied condition (only 3rd scan is shown).Legend: A and E: Scat; B and F: SP1; C and G: SP2; D and H: SP3

Table 1. Overall performance and CV analysis data of each microcosm.

			Microcosms			
			Scat	**SP1**	**SP2**	**SP3**
Chronoamperometry	**Performance during microcosms' inoculation and start-up in medium containing NO_3^-**	**Operation time** (days)	8	5	5	5
		Accumulated charge (C)	3.8	2.2	1.7	2.5
		NO_3^- removed ($mmolNO_3^- \cdot L^{-1}$)	2.35	2.64	1.62	2.78
		$NO_{2\ accumulated}^-/NO_{3\ removed}^-$ (%)	39.8	34.3	54.1	36.9
		CE NO_3^-/NO_2^- (%)	46.9	24.5	30.3	25.7
	Stable current at each applied condition ($\mu A\ cm^{-2}$)	**NO_3^-**	-2.40	-3.60	-3.49	-3.78
		$NO_3^-+NO_2^-$	-1.59	-2.92	-3.09	-3.33
		NO_2^-	-0.51	-0.39	-0.30	-0.22
		Buffer	-0.09	-0.10	-0.10	-0.13
Cyclic voltammetry	**Midpoint redox potentials** (V vs. Ag/AgCl)	**NO_3^-**	-0.28	-0.29	-0.29	-0.27
		$NO_3^-+NO_2^-$	-0.28	-0.29	-0.29	-0.27
			-	-0.71	-0.70	-0.69
		NO_2^-	-0.70	-0.72	-0.66	-0.64

Graphical abstract

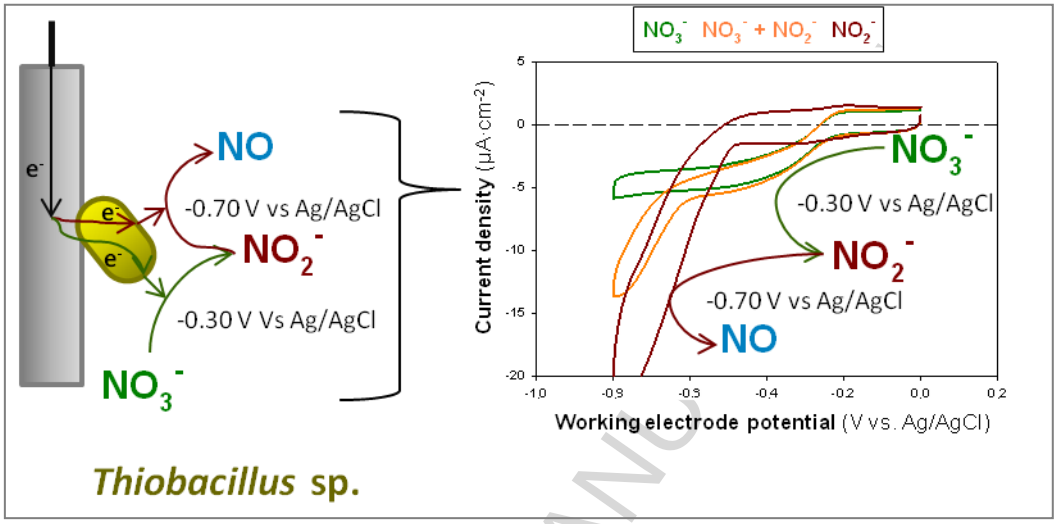

Highlights:

- Microbial microcosms used for characterization of denitrifying microbial cathode(s).
- Thermodynamics for NO_3^- and NO_2^- reduction are revealed by cyclic voltammetry.
- Nitrate and nitrite reduction proceed at -0.30 V and -0.70 V vs. Ag/AgCl, respectively.
- Microbial community is dominated by the electrotroph microorganism *Thiobacillus sp.*